Novel Method for the Measurement of Xenon Gas Solubility Using ^{129}Xe NMR Spectroscopy

Nicolas Segebarth,[†] Lhoucine Aïtjeddig,[†] Emanuela Locci,[‡] Kristin Bartik,[§] and Michel Luhmer*,[†]

Laboratoire de RMN Haute Résolution CP 160/08, Université Libre de Bruxelles, Belgium, Dipartimento di Scienze Chimiche, Università di Cagliari, Italy, and Molecular and Biomolecular Engineering, CP 165/64, Université Libre de Bruxelles, Belgium

Received: May 2, 2006; In Final Form: July 20, 2006

A novel method is presented for determining xenon partitioning between a gas phase and a liquid phase. An experimental setup which permits the simultaneous measurement of the ^{129}Xe chemical shift in both the gas and the liquid phases, that is, under the same experimental conditions, has been designed. Xenon solubility is obtained via ^{129}Xe chemical shift measurements in the gas phase. The method was validated against xenon solubility data from the literature; in general, the agreement is found to be within 3%. The solubility of xenon in three solvents for which data have not been previously reported (acetone, acetonitrile, and 1,1,2,2-tetrachloroethane) was determined using this novel method. ^{129}Xe chemical shifts for dissolved xenon are also reported; it is found that xenon−xenon interactions may play a significant role in the liquid phase even at low equilibrium xenon pressures.

Introduction

The xenon atom possesses a large and highly polarizable electron cloud, and consequently, its local environment strongly affects the chemical shift and relaxation rates of the ^{129}Xe and ^{131}Xe nuclei. Monatomic xenon has therefore been extensively used as a "spin spy" to probe the physicochemical properties of solid, liquid, and gaseous systems.[1−8] Most xenon NMR studies deal with the chemical shift of ^{129}Xe which has been shown to be exquisitely sensitive to the surroundings of the xenon atom and, moreover, is easily measured. ^{129}Xe chemical shift measurements have been used to distinguish and characterize different systems and to study a large variety of processes. For instance, solution state ^{129}Xe NMR has been used to study the intermolecular interactions of xenon atoms with solvent and solute molecules,[9−19] to investigate phase transitions in liquid crystals,[20] to characterize hydrophobic cavities in organic host molecules and proteins,[21−37] to evidence diastereoisomeric structures in chiral recognition processes,[38,39] and to study configurational[40,41] and conformational[42−44] equilibria.

The amount of xenon dissolved in solution is generally required in order to quantitatively characterize the system under study. Solubility data for xenon in several solvents are reported in the literature;[45−49] however, the list is limited and the data are not always available at the desired temperature. Furthermore, solubility data usually refer to pure solvents or simple binary solutions and not to more complex systems that could exhibit an increased affinity for xenon as a consequence, for instance, of xenon trapping.

An experimental method devised to measure, in situ, the partition of xenon in the sample submitted to the NMR experiment is presented here. The method is based on the measurement of the ^{129}Xe chemical shifts in the gas phase, δ_g, in equilibrium with the liquid phase of interest in a sealed NMR tube. In the pure xenon gas phase, xenon−xenon interactions are responsible for the dependence of δ_g on the xenon gas density (i.e., xenon gas pressure); this effect is found to be of the order of 0.5 ppm amagat^{-1} at low xenon pressures and room temperature.[50] (1 amagat corresponds to the density of an ideal gas at STP: 4.462×10^{-2} mol L^{-1}.) For xenon loaded into a sealed tube containing a liquid phase, the value of δ_g primarily reflects the partition of xenon between the gas and liquid phases. The method was tested against a series of seven solvents for which the xenon solubility is known and then applied to measure the solubility of xenon in three solvents for which, to our knowledge, xenon solubility data have never been reported.

The experimental setup used in this work also permits the simultaneous measurement of the ^{129}Xe chemical shift in the liquid phase. ^{129}Xe chemical shift data for dissolved xenon are also reported, and the importance of xenon−xenon interactions in the liquid phase is investigated.

Theoretical Aspects of the Methodology

In the pure gas phase, the shielding constant of an atom can be written as[50,51]

$$\sigma(\rho) = \sigma_0 + \sigma_1\rho + \sigma_2\rho^2 + ... \quad (1)$$

ρ is the density of the gas, σ_0 is the shielding constant of the isolated atom, and σ_1, σ_2, ... account for the effect of pair, three-body, and higher order interactions. These coefficients, and thus also $\sigma(\rho)$, are temperature dependent. At low pressure, the nonlinear terms of this virial expansion are negligible and the chemical shift, referenced to the chemical shift of the pure gas at zero pressure, is simply given by

$$\delta_g = -(\sigma(\rho) - \sigma_0) = -\sigma_1\rho \quad (2)$$

* Corresponding author. Present address: 50 av. F.D. Roosevelt, 1050 Brussels, Belgium. Phone: +32 (0)2 650 66 37. Fax: +32 (0)2 650 66 42. E-mail: michel.luhmer@ulb.ac.be.
[†] Laboratoire de RMN Haute Résolution, Université Libre de Bruxelles.
[‡] Università di Cagliari.
[§] Molecular and Biomolecular Engineering, Université Libre de Bruxelles.

10.1021/jp062679k CCC: $33.50
Published on Web 08/24/2006

For heavy gases such as xenon, the total amount of gas introduced into a sealed NMR tube (loading) can be precisely determined by weighting. It is therefore convenient to rewrite eq 2 as a function of the mass of xenon gas loaded into the NMR tube, m_{Xe}:

$$\delta_g = \beta_0 m_{Xe} \tag{3}$$

with

$$\beta_0 = -\frac{\sigma_{1(Xe-Xe)}}{M_{Xe}V_t} \tag{4}$$

$\sigma_{1(Xe-Xe)}$ is the second coefficient of the virial associated with the xenon−xenon pair interactions, V_t is the experimentally determined inner volume of the NMR tube, and M_{Xe} is the atomic mass of xenon (131.3 g mol^{-1} if natural abundance xenon is used).

For xenon in the presence of other gases, δ_g also depends on the interactions between the xenon atoms and the other species present.[50] In the presence of a pure liquid phase, the interactions between xenon atoms and solvent molecules in the gas phase must therefore be taken into account and δ_g can be written as

$$\delta_g = -(\sigma_{1(Xe-Xe)}\rho_{Xe} + \sigma_{1(Xe-S)}\rho_S) \tag{5}$$

ρ_{Xe} is the density of xenon gas, ρ_S is the density of the solvent in the gas phase, and $\sigma_{1(Xe-S)}$ is the second virial coefficient of the xenon shielding constant that accounts for the effect of xenon−solvent pair interactions in the gas phase. Equation 5 can also be written as a function of the total mass of xenon in the NMR tube (see the Supporting Information):

$$\delta_g = \alpha + \beta m_{Xe} \tag{6}$$

with

$$\alpha = \frac{-\sigma_{1(Xe-S)}P_S}{RT} \tag{7}$$

$$\beta = \frac{\beta_0}{\left(1 + (L-1)\frac{V_l}{V_t}\right)} \tag{8}$$

P_S is the vapor pressure of the solvent, V_l is the volume of the liquid phase, and L is the Ostwald coefficient that describes the partition of xenon between the liquid and gas phases:

$$L = \frac{[Xe]_l}{[Xe]_g} \tag{9}$$

$[Xe]_l$ and $[Xe]_g$ are the molar concentrations of xenon in the liquid phase and the gas phase, respectively. For an equilibrium xenon pressure of 1 atm, assuming ideal behavior, $[Xe]_g = (RT)^{-1}$, that is, 4.01×10^{-2} mol L^{-1} at 298 K.

In the presence of a liquid phase, δ_g is a linear function of the total mass of xenon in the NMR tube provided that volume variations of the liquid phase are negligible (see the Supporting Information). It is worth noting that xenon−solvent interactions only affect the intercept α (eq 7) and that this contribution is not expected to be dominant if the equilibrium xenon pressure is significantly larger than the solvent vapor pressure. Therefore, if $L < 1$, that is, the xenon solubility in the liquid phase is lower than the corresponding concentration of xenon in the gas phase, δ_g will be larger than the value that would be measured in the absence of the liquid phase at identical xenon loading. Conversely, a smaller δ_g value will be measured if $L > 1$. Analysis of δ_g measurements performed at various xenon loadings for pure xenon gas and for xenon in equilibrium with a liquid phase yield the β_0 and β values from which the Ostwald coefficient can be determined using eq 8. The xenon solubility is thus readily obtained using eq 9.

Experimental Methods

High-purity solvents (>99%) were purchased and used as provided. Xenon was purchased from Air Liquide (natural abundance, N48).

The experimental setup consists of a 10 mm high-pressure NMR tube equipped with a valve (Wilmad 513-7PVH) modified in such a way that an open coaxial 5 mm tube, ~8 cm long, is fixed to its bottom. If a liquid phase is present, it is contained in the annular region outside the 5 mm tube. The setup thus permits the simultaneous NMR observation of gaseous xenon (contained in the 5 mm tube) and dissolved xenon. The total inner volume of the modified 10 mm NMR tube, V_t, is 5.786 mL (determined by weighting its water content).

For ^{129}Xe chemical shift measurements in the pure gas phase, the NMR tube was evacuated and xenon was then loaded in order to reach a xenon pressure between 8 and 9 atm. For the successive measurements at lower xenon pressure, xenon was partially evacuated on a vacuum rack. The total amount of xenon in the NMR tube was determined by weighting before the NMR experiment and controlled after the experiment. For the experiments performed in the presence of a solvent, ~1.5 mL of solvent was introduced into the 10 mm NMR tube and thoroughly degassed by several cycles of sonication in an ultrasound bath and evacuation on a vacuum rack. The final volume of solvent in the NMR tube was determined by weighting. Successive loadings of xenon gas were made for these experiments. Here also, the total amount of xenon in the NMR tube was determined by weighting. The NMR tube was laid down horizontally at 25 °C, for 1 h, to increase the gas−liquid interface and left to reach equilibrium. The NMR spectra were recorded after an additional period of equilibration in the spectrometer of at least 30 min. No significant ^{129}Xe chemical shift change was observed in spectra recorded overnight, confirming that the equilibrium was reached.

The ^{129}Xe NMR spectra were recorded at 298.0 ± 0.1 K on a Bruker AMX360 spectrometer (the nominal frequency for ^{129}Xe is 99.64 MHz) equipped with a standard 10 mm broadband probe using a 3 μs pulse (~30°), an acquisition time of 0.5 s, a relaxation delay of 4.5 s, 32 or 64 scans, and a spectral width of 300 ppm centered at approximately 100 ppm. ^{129}Xe chemical shifts were referenced to the resonance frequency of pure xenon gas extrapolated to zero pressure. This value was determined from the pure gas phase ^{129}Xe chemical shift series of measurements and set to zero. A secondary reference consisting of a sealed 10 mm NMR tube containing xenon dissolved in acetone-*d*6 was then calibrated and used for referencing each series of measurements with solvents. The NMR spectra were recorded unlocked. For pure xenon gas experiments, B_0 field homogeneity was reached by shimming on the ^{129}Xe free induction decay (FID) at the highest xenon loading. For the experiments in the presence of a solvent, shimming was performed on the solvent ^{1}H FID at the lowest xenon loading. A referencing spectrum was recorded unlocked under the same shim conditions after the first and last measurement of each series.

Exponential apodization was applied with a line broadening factor of 1 Hz; the digital resolution was 0.2 Hz per point. Line

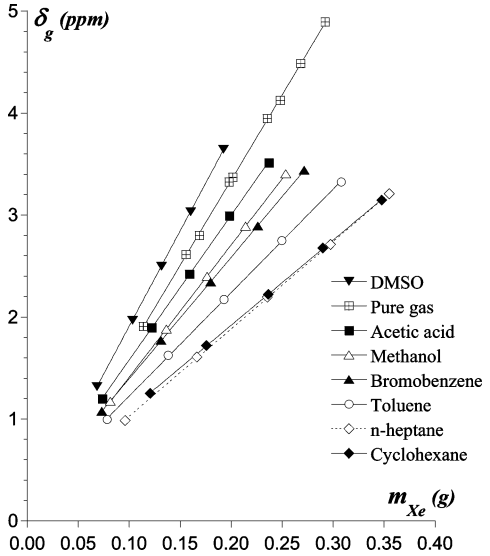

Figure 1. ^{129}Xe chemical shift measured at 298 K in the pure gas phase (xenon pressures lower than 9 atm) and for xenon gas in equilibrium with xenon dissolved in simple solvents (equilibrium xenon pressures lower than 7 atm). m_{Xe} is the mass of the total amount of xenon loaded into the NMR tube. Data points resulting from two independent series of measurements are plotted for the pure xenon gas phase.

widths were typically of the order of a few hertz; the signal-to-noise ratio was higher than 10 for the xenon gas signal and higher than 15 for the dissolved xenon signal.

Results and Discussion

Measurement of Xenon Solubility. ^{129}Xe chemical shifts were measured at various xenon loadings in a sealed NMR tube for pure xenon gas and for xenon in the presence of liquid solvents. All measurements were performed at 298 K using our designed NMR tube (see Experimental Methods).

The variation of δ_g for pure xenon gas as a function of the xenon mass in the NMR tube is shown in Figure 1 where data from two series of independent measurements are presented. In these experiments, the xenon pressure did not exceed 9 atm. As expected for this range of pressures, δ_g increases linearly with xenon loading. The fitting of eq 3 to the experimental data yields the slope β_0 that translates into a $\sigma_{1(Xe-Xe)}$ value of $-(0.566 \pm 0.003)$ ppm amagat^{-1}, that is, $-(12.70 \pm 0.07)$ ppm mol L^{-1} using eq 4. This value is in good agreement with those reported in the literature by Jameson et al.,[50] $-(0.548 \pm 0.004)$ ppm amagat^{-1}, for measurements made between 30 and 110 amagats, and by Brunner and co-workers,[52] $-(0.509 \pm 0.030)$ ppm amagat^{-1}, for measurements made between 40 and 440 amagats, at the same temperature. The intercept, that is, the extrapolation of δ_g to zero loading, was used for chemical shift referencing and set to zero.

The proposed NMR method for xenon gas solubility measurement was tested against seven solvents for which data at 1 atm and 298 K are reported in the literature and range between 0.02 and 0.2 mol L^{-1} (see Table 1). A series of five measurements corresponding to different xenon loadings was performed for each solvent; in these experiments, the xenon pressure did not exceed 7 atm. The variation of δ_g as a function of xenon mass in the NMR tube is apparently linear (see Figure 1). For DMSO, δ_g is larger than the value measured at identical xenon loading in pure xenon gas. This is expected, since the Ostwald coefficient for xenon dissolved in this solvent is lower than 1 (solubility lower than 4.01×10^{-2} mol L^{-1} at 1 atm and 298 K). The parametric adjustment of eq 6 to the experimental δ_g data provides the slopes, β, that can be used to calculate the Ostwald coefficient, and the corresponding xenon solubility, using eqs 8 and 9 and the previously determined β_0 value. The results are reported in Table 1 and shown in Figure 2a where they are compared to data from the literature. A very good agreement is observed, but our data are systematically slightly overestimated for solvents in which xenon solubility is higher than 0.1 mol L^{-1}. Variations of the volume of the liquid phase due to the dissolution of xenon are neglected in the data analysis presented above. If this variation is taken into account, as explained below, our data are in excellent agreement over the entire studied solubility range, as can be seen in Table 1 and Figure 2b.

TABLE 1: Xenon Solubility Data (In This Work, Xenon Solubility Data Are Determined from ^{129}Xe Chemical Shift Measurements in the Gas Phase (See Text); Two Independent Series of Measurements Were Performed for Acetonitrile, Acetone, and 1,1,2,2-Tetrachloroethane)

	xenon solubility (mol L^{-1}) at 298 K and 1 atm			
		this work		
solvent	literature[a]	*b*	*c*	*d*
DMSO	0.024	0.023	0.024	0.022
acetic acid	0.067	0.070	0.069	0.062
methanol	0.086	0.089	0.087	0.082
bromobenzene	0.104	0.108	0.104	0.094
toluene	0.139	0.147	0.140	0.131
heptane	0.184	0.199	0.185	0.182
cyclohexane	0.194	0.208	0.192	0.182
acetonitrile			0.065/0.065	
acetone			0.097/0.100	
1,1,2,2-tetrachloroethane			0.101/0.105	

[a] References 45, 48, and 49. [b] Results determined from four or five measurements at equilibrium xenon pressures lower than 7 atm neglecting liquid phase volume expansion. [c] Results determined from four or five measurements at equilibrium xenon pressures lower than 7 atm taking into account liquid phase volume expansion. [d] Results determined from a single xenon loading measurement (one-shot xenon solubility estimation).

If the partial molar volume of dissolved xenon, as well as the partial molar volume of the solvent molecules in the liquid phase, is considered to be independent of the xenon concentration, the volume of the liquid phase that appears in eq 8 is given by

$$V_l = V_l^\circ + \upsilon_{Xe} n_{Xe(l)} \tag{10}$$

V_l° is the volume of the degassed liquid phase, υ_{Xe} is the partial molar volume of dissolved xenon, and $n_{Xe(l)}$ is the number of moles of dissolved xenon at equilibrium. Equation 10 can be rewritten as a linear function of the total mass of xenon gas in the NMR tube:

$$V_l = V_l^\circ + \kappa m_{Xe} \tag{11}$$

For the xenon concentrations encountered in this work, κ is given by (see the Supporting Information)

$$\kappa = \frac{L}{\frac{V_t}{V_l^\circ} + L - 1} \frac{\upsilon_{Xe}}{M_{Xe}} \tag{12}$$

κ was determined by parametric adjustment of eq 11 to V_l data obtained by measuring the height of the liquid phase in the NMR

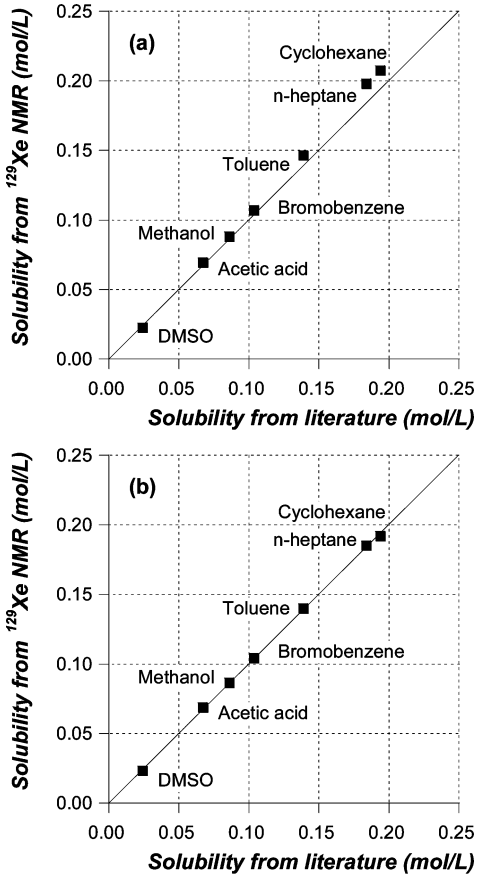

Figure 2. Comparison of the xenon solubility data (298 K, 1 atm) determined by ^{129}Xe NMR to xenon solubility data from the literature;[45,48,49] the line $Y = X$ is drawn in both figures as a guide for the eye. (a) The analysis of ^{129}Xe chemical shift measurements in the gas phase neglects the liquid phase volume expansion. (b) The liquid phase volume expansion is taken into account.

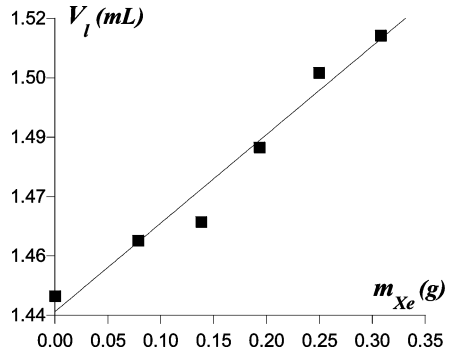

Figure 3. Liquid phase volume variation upon xenon dissolution in toluene. m_{Xe} is the total mass of xenon loaded into the NMR tube. V_l data were obtained by measuring the height of the liquid phase in the NMR tube and the volume of the degassed liquid phase determined using the mass of degassed liquid in the tube and the pure solvent density.

tube at different xenon loadings. All solvents, with the exception of dimethyl sulfoxide (DMSO) and acetic acid, showed volume variations that could be properly estimated in this way. The V_l data obtained for toluene are shown in Figure 3, and the determined κ values are shown in Figure 4.

The partial molar volume of xenon obtained using eq 12 ranges between 56 and 75 cm^3 mol^{-1}. This variation is not significant considering the precision in the liquid phase volume measurements. The average value for υ_{Xe} is found to be 65 ± 7 cm^3 mol^{-1} and accounts correctly for the trend observed in κ values (see Figure 4). This suggests that the liquid phase volume expansion observed as a consequence of xenon dissolution can be accounted for using a solvent independent value for the partial molar volume of dissolved xenon. The xenon solubility data reported in Table 1 and shown in Figure 2b were determined by parametric adjustment of eq 6 to the experimental δ_g data using eqs 8, 11, and 12, the experimentally determined β_0 value, and the average υ_{Xe} value given above. The agreement between our solubility data determined by ^{129}Xe NMR and literature data, usually reported with relative errors between 0.5 and 3%,[45,48,49] is now, as mentioned before, excellent over the whole range of solubility values. The differences are of the order of 2×10^{-3} mol L^{-1}, which corresponds to relative differences smaller than 3%. The method presented here would however probably not be suitable for measuring xenon solubility values lower than 0.01 mol L^{-1}, such as those found for pure water and dilute aqueous systems.

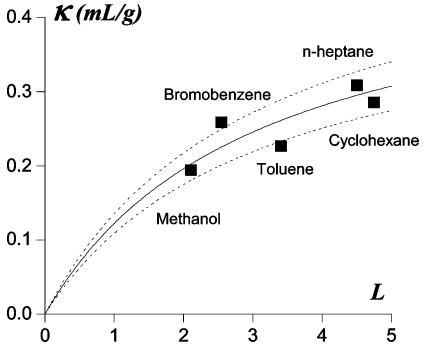

Figure 4. Empirical liquid phase volume expansion coefficient, κ, for xenon dissolution. L is the Ostwald coefficient corresponding to the xenon solubility reported in the literature. In our experiments, the volume of degassed solvent was kept as constant as possible: V_l° ranges between 1.42 and 1.44 mL. The volume of the tube, V_t, is 5.786 mL. The curves represent eq 12 using the average experimental value for V_t/V_l° (i.e., $V_t/V_l^\circ = 4.05$), $\upsilon_{Xe} = 65$ cm^3 mol^{-1} (plain curve) or $\upsilon_{Xe} = 65 \pm 7$ cm^3 mol^{-1} (dotted curves).

^{129}Xe NMR was used to determine the solubility of xenon in three solvents for which, to our knowledge, xenon solubility values are not reported: acetonitrile, acetone, and 1,1,2,2-tetrachloroethane. Two independent series of four measurements at different xenon loadings were performed for each solvent. The xenon solubility values are reported in Table 1.

One-Shot Xenon Solubility Estimation. Precise determination of the xenon solubility by ^{129}Xe NMR requires chemical shift measurements at various xenon loadings, but a single measurement can be used to obtain a good estimate of the solubility. Using eqs 6, 8, and 11, the Ostwald coefficient is given by

$$L = 1 + \left(\frac{\beta_0}{\delta_g - \alpha} m_{Xe} - 1\right)\frac{V_t}{V_l^\circ + \kappa m_{Xe}} \qquad (13)$$

The α values measured in the present study range between 0.0 and 0.4 ppm. α cannot be determined via a single xenon loading experiment, but it is interesting to point out that α and κ have opposite effects on L: neglecting α, which is positive, leads to an underestimation of L, while neglecting κ leads to an overestimation. With good chemical shift referencing, the error introduced on the xenon solubility if α and κ are neglected (eq 14) is relatively small if a xenon loading corresponding to an

TABLE 2: ^{129}Xe Chemical Shift Data at 298 K for Xenon Dissolved in Different Solvents (Two Independent Series of Measurements Were Performed for Acetonitrile, Acetone, and 1,1,2,2-Tetrachloroethane; the Fitting Errors on δ_l° Are Smaller Than ±0.03 ppm, and the Fitting Errors on ξ Are Smaller than ±0.06 ppm mol^{-1} L)

solvent	$\delta_l^\circ = -(1/v_S)\sigma^*_{1(Xe-S)}$ (ppm)	$\xi = -\sigma^*_{1(Xe-Xe)} - v_{Xe}\delta_l^\circ$ (ppm mol^{-1} L)
DMSO	243.24	0.48
acetic acid	158.94	4.18
methanol	142.30	4.41
bromobenzene	212.95	0.91
toluene	184.72	1.69
heptane	162.14	2.39
cyclohexane	159.65	3.04
acetonitrile	170.97/170.97	3.09/3.08
acetone	170.67/170.71	2.01/1.97
1,1,2,2-tetrachloroethane	223.56/223.65	*a*

[a] The ^{129}Xe chemical shift of xenon dissolved in 1,1,2,2-tetrachloroethane is not significantly dependent on the xenon loading for equilibrium xenon pressures lower than 7 atm.

equilibrium xenon pressure between 5 and 10 atm is used (this ensures a δ_g value significantly larger than α).

$$L = 1 + \left(\frac{\beta_0}{\delta_g} m_{Xe} - 1\right)\frac{V_t}{V_l^\circ} \qquad (14)$$

Solubility data determined using eq 14 and the δ_g value measured at the highest xenon loading reached in this work (see Figure 1) are reported in Table 1. For this set of measurements, the differences with the solubility data from the literature are smaller than 10%. It is worth noting that such an estimation of the xenon solubility based on a single measurement leads to a systematic underestimation. It is also worth pointing out that using eq 7 it should be possible to determine $\sigma_{1(Xe-S)}$ data from α values. Experimental $\sigma_{1(Xe-S)}$ data are valuable because they could be used to test the quality of ab initio pair shielding functions. However, the experimental setup designed for solubility measurements and the experimental conditions used in this work are not suitable for precise measurements of $\sigma_{1(Xe-S)}$. The measured α values are less than 0.4 ppm, and two independent measurements may lead to a difference of 0.1 ppm. Therefore, the measured α values are not reported nor discussed.

Xenon−Xenon Interactions in the Liquid Phase. The designed experimental setup has the advantage of allowing the simultaneous measurement of the ^{129}Xe chemical shift in both the gas phase and the liquid phase. In liquid state ^{129}Xe NMR studies, the xenon is frequently assumed to be infinitely diluted and the effect of xenon−xenon interactions is usually neglected.[4] However, we previously reported that xenon−xenon interactions may contribute significantly to ^{129}Xe chemical shift data measured for dissolved xenon under pressures lower than 10 atm.[44] In the present work, the chemical shift of ^{129}Xe dissolved in the liquid solvents, δ_l, was also measured at various xenon loadings. The chemical shift values extrapolated to zero xenon pressure, δ_l°, are reported in Table 2, and the variations of δ_l with xenon loading, which is apparently linear, are shown in Figure 5.

For equilibrium xenon pressures lower than 7 atm, no significant variation of δ_l with xenon loading was found for xenon dissolved in 1,1,2,2-tetrachlotoethane (not shown) and a weak increase of δ_l was observed for xenon in DMSO (see Figure 5). However, in the same range of equilibrium xenon pressures, the variation of δ_l is of the order of 3.5 ppm for xenon dissolved in cyclohexane. Our results show that in most of the solvents studied the ^{129}Xe chemical shift, even at the lowest

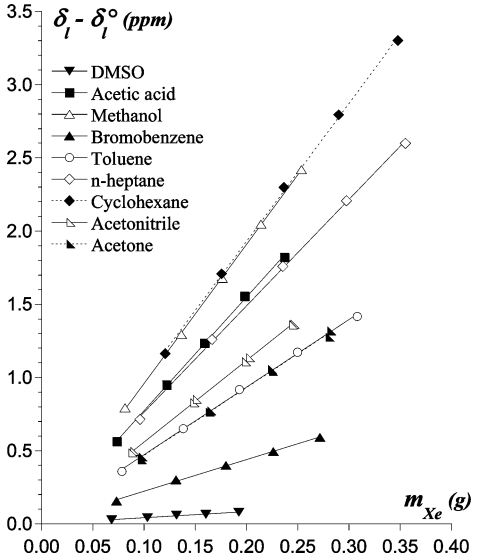

Figure 5. Variation with xenon loading of the ^{129}Xe chemical shift measured at 298 K for xenon dissolved in different solvents. m_{Xe} is the total mass of xenon loaded into the NMR tube; the corresponding equilibrium xenon pressures are lower than 7 atm. Data points resulting from two independent series of measurements are plotted for xenon dissolved in acetonitrile and acetone.

xenon loading used, is significantly higher than the value extrapolated to zero xenon pressure; a low-field shift ranging between 0.3 and 0.6 ppm is typically observed (Figure 5). Considering that these effects are primarily a consequence of xenon−xenon interactions in the liquid phase, the variation of δ_l with xenon loading is expected to be large for solvents in which xenon is highly soluble. Solubility differences by themselves cannot however explain the experimental data. The variation of δ_l with xenon loading is found to be similar in cyclohexane and methanol, while the solubility of xenon is more than twice as large in cyclohexane (see Table 1). Furthermore, no significant variation of δ_l was observed in 1,1,2,2-tetrachloroethane, although the xenon solubility in this solvent is larger than that in methanol. Obviously, the observed effect depends on the relative contribution of xenon−xenon interactions and xenon−solvent interactions to the shielding of ^{129}Xe. In the framework of an additive pair contribution model, the chemical shift of dissolved ^{129}Xe at low xenon pressure can be written, similarly to eq 5, as

$$\delta_l = -\left(\sigma^*_{1(Xe-Xe)}\frac{n_{Xe(l)}}{V_l} + \sigma^*_{1(Xe-S)}\frac{n_{S(l)}}{V_l}\right) \qquad (15)$$

$n_{Xe(l)}$ is the number of moles of dissolved xenon at equilibrium, $n_{S(l)}$ is the number of moles of solvent molecules in the liquid phase, and $\sigma^*_{1(Xe-Xe)}$ and $\sigma^*_{1(Xe-S)}$ are the contributions to the ^{129}Xe shielding due to xenon−xenon and xenon−solvent pair interactions in the liquid phase. It is worth noting that $\sigma^*_{1(Xe-Xe)}$ depends on the xenon−xenon pair distribution function which, in the liquid phase, also depends on xenon−solvent and solvent−solvent interactions. The ^{129}Xe chemical shift extrapolated to zero xenon pressure is given by

$$\delta_l^\circ = -\sigma^*_{1(Xe-S)}\frac{n_{S(l)}}{V_l^\circ} = -\frac{\sigma^*_{1(Xe-S)}}{v_S} \qquad (16)$$

where v_S is the partial molar volume of the solvent molecules in the liquid phase. Assuming that the partial molar volume of dissolved xenon and the partial molar volume of the solvent

molecules are independent of the xenon concentration, eq 15 can be transformed into (see the Supporting Information)

$$\delta_l = \delta_l^\circ + \xi[Xe]_l \quad (17)$$

with

$$\xi = -\sigma^*_{1(Xe-Xe)} + \frac{v_{Xe}}{v_S}\sigma^*_{1(Xe-S)} = -\sigma^*_{1(Xe-Xe)} - v_{Xe}\delta_l^\circ \quad (18)$$

$$[Xe]_l = \frac{L}{\left(1 + (L-1)\frac{V_l}{V_t}\right)}\frac{1}{V_t}\frac{m_{Xe}}{M_{Xe}} \quad (19)$$

The ξ data reported in Table 2 were determined by parametric adjustment of eqs 17 and 19 to the experimental δ_l data using eqs 11 and 12 for V_l and $v_{Xe} = 65$ cm^3 mol^{-1}. The use of a v_{Xe} value smaller or larger by 30% does not significantly affect the values determined for ξ. Errors on v_{Xe} do however directly affect $\sigma^*_{1(Xe-Xe)}$ values that are calculated using eq 18 and the experimentally determined ξ data. Despite the uncertainty on v_{Xe}, $\sigma^*_{1(Xe-Xe)}$ ranges between -12.9 and -14.7 ppm mol L^{-1} (DMSO excluded) and is found to be similar to $\sigma_{1(Xe-Xe)}$, which accounts for the shielding effect of xenon−xenon pair interactions in the gas phase ($\sigma_{1(Xe-Xe)} = -12.70$ ppm mol L^{-1}).

Conclusion

The ^{129}Xe chemical shift of xenon in the gas phase is dependent on xenon pressure. The present work demonstrates that this property can be used to determine the xenon partition between a gas and a liquid phase, that is, the xenon solubility in liquids. In this study, xenon solubility data in pure solvents were determined by ^{129}Xe NMR. If the liquid phase volume expansion due to xenon dissolution is taken into account, using a solvent independent value for the partial molar volume of dissolved xenon, an excellent agreement is found with data from the literature. The agreement with data from the literature is however still extremely good if this correction is neglected. Furthermore, if only an estimate of xenon solubility is needed, it is possible to obtain it running a simple one-load experiment.

The NMR tube designed for this work permits the simultaneous observation of xenon in the gas phase and in the liquid phase, that is, under the same experimental conditions. This gives the method its real interest, since it permits the determination in situ of the concentration of dissolved xenon used in solution state ^{129}Xe NMR studies. It is illustrated in this work by investigating the xenon concentration dependence of the ^{129}Xe chemical shift of dissolved xenon. For the first time, this effect is characterized quantitatively. It is shown to be dependent on the relative contribution of xenon−xenon and xenon−solvent interactions to the ^{129}Xe chemical shift, and the contribution of xenon−xenon pair interactions in the liquid phase is estimated. The analysis explains why in some solvents the ^{129}Xe chemical shift is found to be essentially constant for equilibrium xenon pressures lower than 10 atm while in others the effect is of the range of a few parts per million.

Acknowledgment. The authors thank the "Communauté française de Belgique" (ARC 2002-2007 n°286 and 289) and the VII Executive Program for Belgium-Italy Scientific Cooperation 2005-2006 for financial support.

Supporting Information Available: The mathematical developments leading to the major equations used in this work for interpreting the experimental data: (i) the transformation of eq 5 into eqs 6−8, (ii) the transformation of eq 10 into eqs 11 and 12, and (iii) the transformation of eq 15 into eqs 17−19. This material is available free of charge via the Internet at http://pubs.acs.org.

References and Notes

(1) Bartik, K.; Choquet, P.; Constantinesco, A.; Duhamel, G.; Fraissard, J.; Hyacinthe, J.; Jokisaari, J.; Locci, E.; Lowery, T.; Luhmer, M.; Meersmann, T.; Moudrakovski, I.; Pavlovskaya, G.; Pierce, K.; Pines, A.; Ripmeester, J.; Telkki, V.; Veeman, W. *Actual. Chim.* **2005**, *287*, 16.
(2) Dybowski, C.; Bansal, N.; Duncan, T. M. *Annu. Rev. Phys. Chem.* **1991**, *42*, 433.
(3) Raftery, D.; Chmelka, B. F. Xenon NMR Spectroscopy. In *NMR Basic Principles and Progress*; Blümich, B., Ed.; Springer-Verlag: Berlin, Heidelberg, 1994; Vol. 30, p 111.
(4) Ratcliffe, C. I. *Annu. Rep. NMR Spectrosc.* **1998**, *36*, 124.
(5) Reisse, J. *New J. Chem* **1986**, *10*, 665.
(6) Walton, J. H. *Polym. Polym. Compos.* **1994**, *2*, 35.
(7) Barrie, P. J.; Klinowski, J. *Prog. Nucl. Magn. Reson. Spectrosc.* **1992**, *24*, 91.
(8) Bonardet, J.-L.; Fraissard, J.; Gedeon, A.; Springuel-Huet, M.-A. *Catal. Rev.—Sci. Eng.* **1999**, *41*, 115.
(9) Miller, K. W.; Reo, N. V.; Schoot Uiterkamp, A. J. M.; Stengle, D. P.; Stengle, T. R.; Williamson, K. L. *Proc. Natl. Acad. Sci. U.S.A.* **1981**, *78*, 4946.
(10) Moschos, A.; Reisse, J. *J. Magn. Res.* **1991**, *95*, 603.
(11) Stengle, T. R.; Reo, N. V.; Williamson, K. L. *J. Phys. Chem.* **1981**, *85*, 3772.
(12) Stengle, T. R.; Hosseini, S. M.; Basiri, H. G.; Williamson, K. L. *J. Solution Chem.* **1984**, *13*, 779.
(13) Stengle, T. R.; Hosseini, S. M.; Williamson, K. L. *J. Solution Chem.* **1986**, *15*, 777.
(14) Lim, Y. H.; King, A. D. *J. Phys. Chem.* **1993**, *97*, 12173.
(15) Lim, Y.-H.; Nugara, N.; King, A. D. J. *Appl. Magn. Reson.* **1995**, *8*, 521.
(16) Lim, Y.-H.; Calhoun, A. R.; King, A. D. J. *Appl. Magn. Reson.* **1997**, *15*, 555.
(17) Calhoun, A. R.; King, A. D. J. *Appl. Magn. Reson.* **1998**, *15*, 95.
(18) Luhmer, M.; Bartik, K. *J. Phys. Chem. A* **1997**, *101*, 5278.
(19) Luhmer, M.; Dejaegere, A.; Reisse, J. *Magn. Reson. Chem.* **1989**, *27*, 950.
(20) Jokisaari, J. *NMR of noble gases dissolved in liquid crystals*; Burnell, E. E., de Lange, C. A., Eds.; Kluwer: Dordrecht, The Netherlands, 2003; p 109.
(21) Bartik, K.; Luhmer, M.; Dutasta, J. P.; Collet, A.; Reisse, J. *J. Am. Chem. Soc.* **1998**, *120*, 784.
(22) Bartik, K.; Luhmer, M.; Heyes, S. J.; Ottinger, R.; Reisse, J. *J. Magn. Reson., Ser. B* **1995**, *109*, 164.
(23) El Haouaj, M.; Luhmer, M.; Ho Ko, Y.; Kim, K.; Bartik, K. *J. Chem. Soc., Perkin Trans. 2* **2001**, *2*, 804.
(24) El Haouaj, M.; Luhmer, M.; Young, H. K.; Kim, K.; Bartik, K. *J. Chem. Soc., Perkin Trans. 2* **2001**, *2*, 2104.
(25) Luhmer, M.; Goodson, B. M.; Song, Y.-Q.; Laws, D. D.; Kaiser, L.; Cyrier, M. C.; Pines, A. *J. Am. Chem. Soc.* **1999**, *121*, 3502.
(26) Brotin, T.; Lesage, A.; Emsley, L.; Collet, A. *J. Am. Chem. Soc.* **2000**, *122*, 1171.
(27) Locci, E.; Casu, M.; Saba, G.; Lai, A.; Reisse, J.; Bartik, K. *ChemPhysChem* **2002**, *3*, 812.
(28) Locci, E.; Dehouck, Y.; Casu, M.; Saba, G.; Lai, A.; Luhmer, M.; Reisse, J.; Bartik, K. *J. Magn. Reson.* **2001**, *150*, 167.
(29) Rubin, S. M.; Lee, S. Y.; Ruiz, E. J.; Pines, A.; Wemmer, D. E. *J. Mol. Biol.* **2002**, *322*, 425.
(30) Dubois, L.; Parrès, S.; Huber, J. G.; Berthault, P.; Desvaux, H. *J. Phys. Chem. B* **2004**, *108*, 767.
(31) Branda, N.; Grotzfeld, R. M.; Valdes, C.; Rebek, J. *J. Am. Chem. Soc.* **1995**, *117*, 85.
(32) Robbins, T. A.; Knobler, C. B.; Bellew, D. R.; Cram, D. J. *J. Am. Chem. Soc.* **1994**, *116*, 111.
(33) Tilton, R. F. J.; Kuntz, I. D. J. *Biochemistry* **1982**, *21*, 6850.
(34) Landon, C.; Berthault, P.; Vovelle, F.; Desvaux, H. *Prot. Sci.* **2001**, *10*, 762.
(35) Rubin, S. M.; Spence, M. M.; Goodson, B. M.; Wemmer, D. E.; Pines, A. *Proc. Natl. Acad. Sci. U.S.A.* **2000**, *97*, 9472.
(36) Rubin, S. M.; Spence, M. M.; Pines, A.; Wemmer, D. E. *J. Magn. Reson.* **2001**, *152*, 79.
(37) Bowers, C. R.; Storhaug, V.; Webster, C. E.; Bharatam, J.; Cottone, A., III; Gianna, R.; Betsey, K.; Gaffney, B. J. *J. Am. Chem. Soc.* **1999**, *121*, 9370.
(38) Bartik, K.; El Haouaj, M.; Luhmer, M.; Collet, A.; Reisse, J. *ChemPhysChem* **2000**, *1*, 221.

(39) Bartik, K.; Luhmer, M.; Collet, A.; Reisse, J. *Chirality* **2001**, *13*, 2.
(40) Spence, M. M.; Ruiz, E. J.; Rubin, S. M.; Lowery, T. J.; Winssinger, N.; Schultz, P. G.; Wemmer, D. E.; Pines, A. *J. Am. Chem. Soc.* **2004**, *126*, 15287.
(41) Locci, E.; Reisse, J.; Bartik, K. *ChemPhysChem* **2003**, *4*, 305.
(42) Lowery, T.; Doucleff, M.; Ruiz, E. J.; Rubin, S. M.; Pines, A. *Prot. Sci.* **2005**, *14*, 848.
(43) Rubin, S. M.; Spence, M. M.; Dimitrov, I. E.; Ruiz, E. J.; Pines, A.; Wemmer, D. E. *J. Am. Chem. Soc.* **2001**, *123*, 8616.
(44) Locci, E.; Bartik, K.; Segebarth, N.; Luhmer, M.; Reisse, J. *J. Phys. Org. Chem.* **2004**, *17*, 787.
(45) Pollack, G. L. *J. Chem. Phys.* **1981**, *75*, 5875.
(46) Pollack, G. L.; Himm, J. F.; Enyeart, J. J. *J. Chem. Phys.* **1984**, *81*, 3239.
(47) Pollack, G. L.; Kennan, R. P.; Himm, J. F. *J. Chem. Phys.* **1989**, *11*, 6569.
(48) Ben-Naim, A.; Marcus, Y. *J. Chem. Phys.* **1984**, *80*, 4438.
(49) Clever, L. *Solubility Data Series*; Pergamon Press: New York, 1979; Vol. 2.
(50) Jameson, A. K.; Jameson, C. J.; Gutowsky, H. S. *J. Chem. Phys.* **1970**, *53*, 2310.
(51) Jameson, C. J. *Chem. Rev.* **1991**, *91*, 1375.
(52) Baumer, D.; Fink, A.; Brunner, E. *Z. Phys. Chem.* **2003**, *217*, 289.